Journal of Power and Energy Engineering, 2024, 12, 99-114
https://www.scirp.org/journal/jpee
ISSN Online: 2327-5901
ISSN Print: 2327-588X

Properties of Ti-Based Hydrogen Storage Alloy

Rui Xu, Tao Cheng, Chaoyu Li, Xue Yang*, Junfeng Rong*

Sinopec Research Institute of Petroleum Processing Co., Ltd., Beijing, China
Email: xurui.ripp@sinopec.com, *yangx.ripp@sinopec.com, *rongjf.ripp@sinopec.com

How to cite this paper: Xu, R., Cheng, T., Li, C.Y., Yang, X. and Rong, J.F. (2024) Properties of Ti-Based Hydrogen Storage Alloy. *Journal of Power and Energy Engineering*, **12**, 99-114.
https://doi.org/10.4236/jpee.2024.123007

Received: March 11, 2024
Accepted: March 26, 2024
Published: March 29, 2024

Abstract

An efficient and safe hydrogen storage method is one of the important links for the large-scale development of hydrogen in the future. Because of its low price and simple design, Ti-based hydrogen storage alloys are considered to be suitable for practical applications. In this paper, we review the latest research on Ti-based hydrogen storage alloys. Firstly, the machine learning and density functional theory are introduced to provide theoretical guidance for the optimization of Ti-based hydrogen storage alloys. Then, in order to improve the hydrogen storage performance, we briefly introduce the research of AB type and AB2 type Ti-based alloys, focusing on doping elements and adaptive after treatment. Finally, suggestions for the future research and development of Ti-based hydrogen storage alloys are proposed.

Keywords

Renewable Energy, Hydrogen Storage, Ti-Based Alloy, Machine Learning

1. Introduction

With growing energy demand and the need for ecological and environmental protection, the development of clean and renewable new energy is crucial [1] [2]. Hydrogen, as an energy carrier, has high quality energy density (142 MJ/kg) [3] [4] [5]. The safe and efficient storage and transportation of hydrogen is the key to the industrialization of hydrogen energy. The lack of suitable hydrogen storage and transportation methods restricts the large-scale application of hydrogen energy. The solid hydrogen storage system has the advantages of good safety (hydrogen absorption/discharge platform < 1 MPa) and high-volume hydrogen storage density [6] [7].

As shown in **Figure 1**, after years of research, various of solid hydrogen storage materials have been researched, including metal alloys [8] [9] [10], chemical

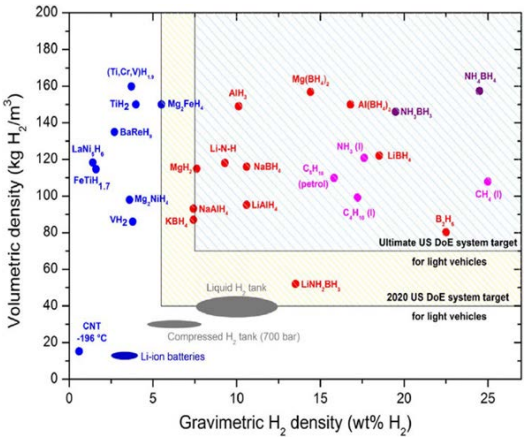

Figure 1. Overview of some MH with their volumetric and gravimetric H-density [17].

hydrides [11] [12] [13], porous materials [14] [15] [16], etc. At present, only hydrogen storage alloys [17] have been applied in practice on a large scale. The practical application of hydrogen storage alloy pressure range 1 - 40 atm and temperature range 273 – 333 k [18].The hydrogen storage principle of hydrogen storage alloys is to reversibly form metal hydrides with hydrogen, or hydrogen and alloy form compounds, that is, gaseous hydrogen molecules are decomposed into hydrogen atoms and enter the metal [19].

Given the benefits of low price, fast hydrogen storage and release rate, and long cycle life of Ti-based hydrogen storage alloy, it is considered to be one of the most likely hydrogen storage alloy materials to be applied in practice. Ti-based hydrogen storage alloys include TiFe [20], $TiMn_2$ [21], $TiCr_2$ [22] etc. It has become more and more necessary in recent years to find alloys with large hydrogen storage capacities, and scientists are dedicated to advancing the technology to store hydrogen at room temperature. In order to satisfy the alloy's application requirements, variety of methods have been obtained to optimized the Ti-based alloys hydrogen storage properties.

2. Properties of Ti-Based Hydrogen Storage Alloys

The Ti-based hydrogen storage alloy includes alloys such as TiFe, $TiMn_2$, and $TiCr_2$. Among them, the representative AB type titanium hydrogen storage alloy is the CsCl structured TiFe alloy, which exhibits a theoretical hydrogen storage capacity of 1.86% (mass fraction) and an equilibrium hydrogen pressure of 0.3 MPa at room temperature. However, its initial activation presents challenges and it is susceptible to gas impurity poisoning. Additionally, the low equilibrium pressure at room temperature may result in hydride instability. Apart from the AB type TiFe alloy, other Ti-basedhydrogen storage materials demonstrate exceptional performance as AB2 types.

2.1. Prediction of Ti-Based Hydrogen Storage Alloys Properties

Due to the complexity of the composition, it is a great challenge to design Ti-

based hydrogen storage alloys with a variety of target properties with excellent performance. With the development of machine learning, the corresponding data are used to model and simulate the composition and crystal phase structure of hydrogen storage materials. The organic combination of machine learning and hydrogen storage alloys plays an important role in promoting the progress of hydrogen storage materials.

In **Figure 2(A)** by using the data-driven innovation method of ensemble learning, the structure-property relationship of Ti-based hydrogen storage alloy is constructed by covering the composition and the characteristics of various crystals. The model can be constructed correctly to predict hydrogen storage capacity in a fast and accurate manner. High-performance hydrogen storage alloys can be logically created in the future using the current concepts [25].

In addition, the hydrogen storage properties of Ti-based alloy is studied by first principles density functional theory simulation. The hydrogenation enthalpy of hydrogen storage alloy is influenced by factors such as electronegativity, atomic radius, and covalent radius. As shown in **Figure 2(B)** through simulations, it is found that higher electronegativity, larger atomic radius and smaller covalent radius, resulting in larger values of hydride enthalpy change. Density functional theory simulations offer insights that can guide the optimization of performance for AB2 Ti-based hydrogen storage alloy [23] [26]. Fadonougbo *et al*. [24] investigated the effect of elemental substitution on the lattice contraction/expansion of TiFe1-xMx alloys and subsequent monohydride decomposition energy using first-principles density functional (DFT) theory calculation with Al, Be, Co, Cr, Cu, Mn, and Ni as substitutional elements for Fe sites. As shown in **Figure 2(C)**, A linear relationship between monohydride formation energy/enthalpy and plateau pressure was proposed.

Machine learning (ML) has been used to discover and optimize the properties of energy-related materials, including hydrogen storage alloys. **Figure 3(A)** illustrates that The overall process of machine learning. Zhou *et al*. [27] utilized ML to identify the most critical factors affecting the hydrogen storage capacity of alloys by ranking the feature importance, instead of through time-consuming and

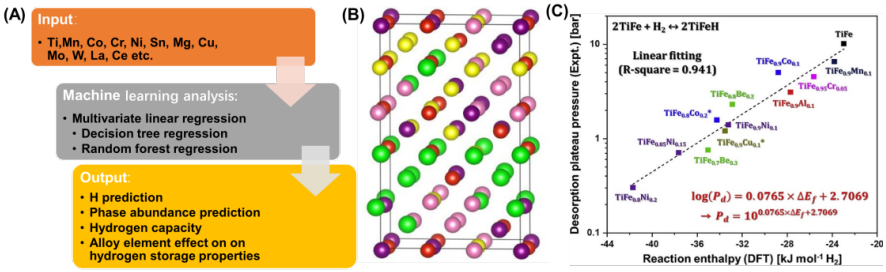

Figure 2. (A) Illustration of steps and analysis during the study; (B) Schematic view of the geometrical structure of BCC Ti-based alloy. The purple, green, red, yellow and pink spheres represent Ti, Zr, V, Mo and Nb atoms, respectively [23]; (C) The correlation between the experimentally measured desorption plateau pressure (at 50˚C) and dehydrogenation enthalpy of single-element alloyed TiFe [24].

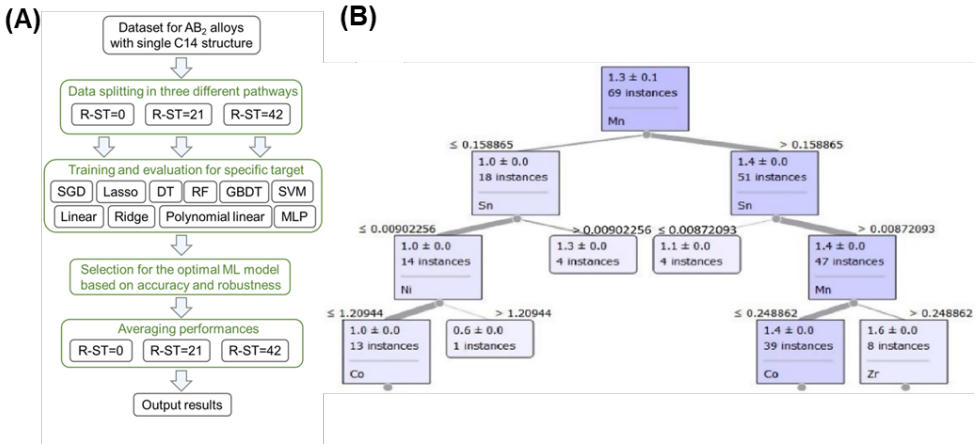

Figure 3. (A) Overall machine learning process [25]; (B) Decision tree-based regression of element effects on hydrogen capacity [26].

costly trial-and-error means to optimize alloy's composition and performance. $Ti_{0.9}Zr_{0.12}Mn_{1.2}Cr_{0.55}(VFe)_{0.25}$ using this algorithm exhibits comprehensive performance (1.90 wt.%/127.30 kgH_2/m^3 saturated state) and overwhelming cost effectiveness at moderate temperature and pressure levels. As shown in **Figure 3(B)**, Suwarno *et al.* [28] used ML approaches to analyze the AB2 metal hydrides dataset. The random forest model accurately forecasts the hydrogen storage properties of the dataset. This paper found that nickel made the largest impact on the enthalpy change of hydride formation while decreasing the hydrogen content. Chromium plays a significant role in the formation of the C14-type Laves phase. Manganese has a notable influence on the hydrogen storage capacity. This research is anticipated to direct future experimental efforts in enhancing the phase structure of AB2 and its hydrogen sorption characteristics

2.2. AB Hydrogen Storage Alloys

TiFe reacted with hydrogen to form $TiFeH_{1.04}$ and $TiFeH_{1.95}$, with hydrogen storage capacity of 1.8 wt%. What's illustrated in **Figure 4(A)** that with different content of Feand Ti, the bulk phase contains different kinds of phases [29]. With a Ti concentration ranging from 49.7 to 52.5 at. %, the single-phase area of TiFe is narrowwith the broadest point occurring at the eutectic temperature of 1085 °C. As shown in **Figure 4(B)**, TiFe crystallizes in cubic CsCl-type structure. The hydrogenation of TiFe results in the formation of $TiFeH_{1.04}$ (possessing an orthorhombic structure with a P_{2221} space group) and $TiFeH_{1.95}$ (possessing an orthorhombic structure with a Cmmm space group) [30]. After activation treatment, TiFe can reversibly absorb or desorb hydrogen at room temperature while $TiFe_2$ does notreact with hydrogen. However, the activation requirements for AB TiFe alloy are still stringent, with an exceeding 723 K temperature and with a range of 5 to 8 MPa pressure needed for complete activation. The incubation time ranges from 10 to 120 minutes, while the recommended number of activation cycles is between 5 and 10. These factors present practical challenges in

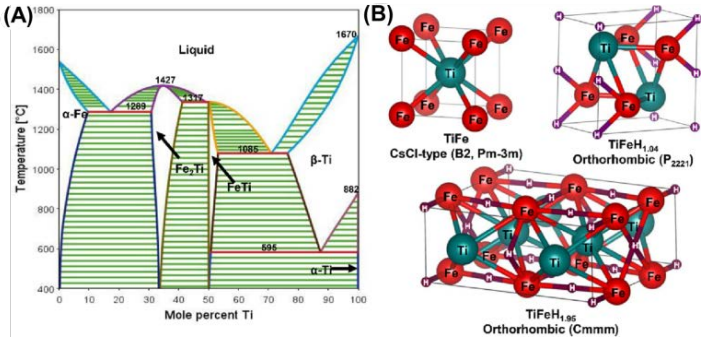

Figure 4. (A) Phase diagram of binary Ti-Fe system [29]; (B) Crystal structures of TiFe, $TiFeH_{1.04}$ and $TiFeH_{1.95}$ [30].

application. To address these limitations, transition elements are frequently employed as partial substitutes for TiFealloy [31] [32], resulting in the formation of multi-element alloys that enable activation at ambient temperatures. In order to enhance the hydrogen storage performance of TiFe alloy, it is typically necessary to modify it through methods such as doping other elements and surface treatment.

In order to enhance the hydrogen storage performance of TiFe alloy, it is typically necessary to modify it through methods such as doping other elements and surface treatment. Incorporating transition metal elements (Co, Cr, Mn, Ni, V, Zr, etc.) into the TiFe alloy by replacing or partially substituting Fe or Ti can effectively improve the activation performance of the alloy to varying degrees and enhance its resistance against toxicity while mitigating the hysteresis effect. However, this modification may result in an increase in the slope of hydrogen absorption and desorption platform for certain alloys and a reduction in their maximum hydrogen storage capacity.

Pati *et al*. [29] researched that the addition of Mn has been discovered to significantly enhance the activation properties of Ti-Fe alloys, with the level of activation rising (the incubation period of first hydrogen absorption decreasing) as the Mn content increases. This improvement is attributed to the catalytic role of Mn in the dissociative chemisorption of H_2, with increasing in the diffusion of H_2 into $TiFe_{1-X}Mn_X$ alloys. what's obvious shown in **Figure 5**, XPS image analysis revealed that the presence of higher Mn concentration effectively inhibited the oxidation of Fe. This observation provides evidence that Mn acts as a sacrificial element, effectively safeguarding Fe from oxidation. Consequently, the inclusion of Mn in the TiFe alloy exhibits a synergistic effect, leading to enhanced hydrogen storage performance.

Liu *et al*. [32] investigated the effect of Nb alloying on the microstructure and hydrogen storage properties of Ti-Fe-Zr-Mn-Nb_x (x = 0, 2, 4, 8 at%) alloys. Nb addition lowers the first plateau pressure and decreases the hysteresis of the isotherms, considering that Nb favors the formation of the TiFe main phase, leading to higher capacities at ambient temperature. Nevertheless, large Nb addition (>4 at%) reduces the activation kinetics through decreasing the Zr-rich phases.

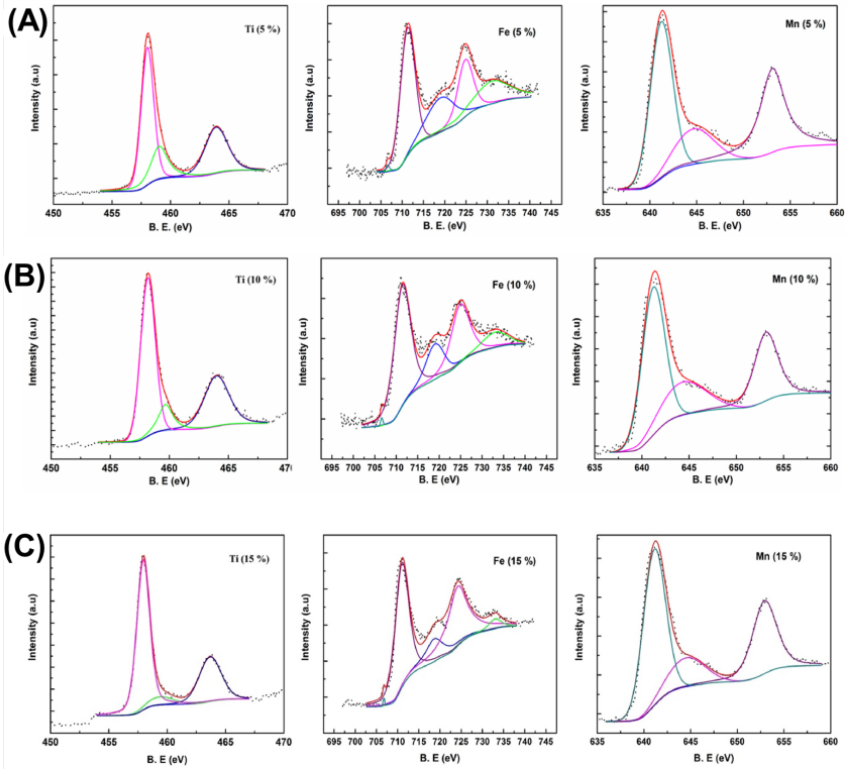

Figure 5. XPS spectra of (A) $TiFe_{0.95}Mn_{0.05}$, (B) $TiFe_{0.90}Mn_{0.1}$ and (C) $TiFe_{0.85}Mn_{0.15}$ alloys after air exposure for 24 h [29].

On account of Li *et al.* [33] research $Ti_{1.08}Y_{0.02}Fe_{0.8}Mn_{0.2}Zr_{0.04}$ alloy hydrogen storage property, finding that the Zr-doped TiFe alloy can be directly activated without the incubation period and decrease the reaction platform pressure for hydrogen storage and release.

Besides, the addition of Cr improves the cycling stability of the alloy material, reduces pulverization, enhances the activation performance of TiFe alloy, and decreases the platform pressure for hydrogen absorption and release [30]. Ce added into AB-type $Ti_{50}Fe_{48}V_2$ significantly improved the hydrogen absorption kinetics of the alloys at room temperature in situations where slow and difficult initial hydrogen absorption is known to be a significant drawback of AB-type hydrogen storage alloys because of their passivating surface oxide layers[34].

2.3. AB2 Hydrogen Storage Alloys

AB2 Ti-based hydrogen storage alloys, $TiCr_2$ and $TiMn_2$ are one of the most widely studied hydrogen storage alloys. AB2 (including $TiCr_2$ [35] and $TiMn_2$ [36] *et al.*) Ti-based hydrogen storage alloy has the advantages of large hydrogen storage capacity, wide range of alloy sources and low price and good kinetic properties.

$TiCr_2$ alloy has characteristics of good resistance to toxicity, while also possess of high platform pressure, large hysteresis effect and low hydrogen absorption temperature. Meanwhile, $TiMn_2$ alloy has a low plateau slope, whereas having a

relatively weak ability of resisting impurity gas poisoning. Therefore, the corresponding optimization was carried out according to the characteristics of $TiCr_2$ alloy and $TiMn_2$ alloy in order to meet the actual production requirements.

2.3.1. Ti-Cralloy

$TiCr_2$ (hexagonal $MgZn_2$ type) is a typical representative of Ti-Cr-based hydrogen storage alloy. Depending on the atomic ratio and position of Ti and Cr, its structure changes between C14 and C15 or two phases occur simultaneously [26]. Partially replacing Ti and Cr in $TiCr_2$ hydrogen storage alloy with chemical elements can increase the hydrogen storage capacity of the alloy or improve the kinetics of hydrogen uptake and desorption of the material.

Xue *et al*. [38] dopped Ce into $TiCr_3V_{16}$ as shown in **Figure 6(A)** & **Figure 6(B)**, illustrated that the pressure-composition-temperature (PCT) test showed that the hydrogen storage plateau pressure of the Ce-doped alloy is increased compared to the Ce-free counterparts, while the hydrogen storage capacity decreased slightly with increasing Ce content. The research developed a $TiCr_3V_{16}Ce_{0.2}$ alloy, as shown in **Figure 6(C)**, which showed a hydrogen absorption rate of up to 3.69 wt.%, and an effective hydrogen desorption capacity of 2.29 wt.% at 25˚C. After hydrogen absorption and desorption cycles, the alloy almost maintains its original capacity. The addition of rare earth elements enlarged the unit cell of $TiCr_2$ alloy, reduced the platform pressure of hydrogen absorption/desorption, and improved the hydrogen storage capacity. Yao *et al*. [37] dopped rare earth (RE) element in the $Ti_{1.02}Cr_{1.1}Mn_{0.3}Fe_{0.6}$ alloy, intended to enhance the activation behavior of alloy with high hydrogen desorption pressure for hybrid hydrogen storage vessel application. After RE doping, the $Ti_{1.02}Cr_{1.1}Mn_{0.3}Fe_{0.6}Re_{0.03}$ alloy exhibits an obviously enhanced activation behavior, with an increase in hydrogen storage capacity and a drop in the hydrogen

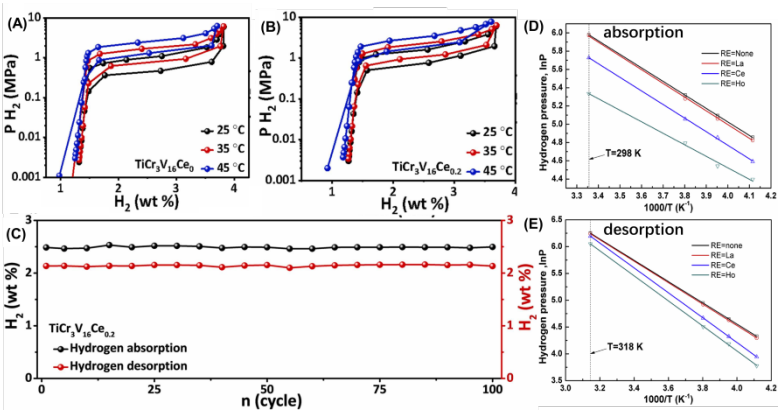

Figure 6. (A) Hydrogen absorption-desorption isotherm $TiCr_3V_{16}Ce_{0.0}$alloy; (B) Hydrogen absorption-desorption isotherm $TiCr_3V_{16}Ce_{0.2}$ alloy; (C) Hydrogen capacity of $TiCr_3V_{16}Ce_{0.2}$ alloy under different cycles at 25˚C. (D) The absorption Van't Hoff plots of $Ti_{1.02}Cr_{1.1}Mn_{0.3}Fe_{0.6}$ and $Ti_{1.02}Cr_{1.1}Mn_{0.3}Fe_{0.6}RE_{0.03}$ (RE = La, Ce, Ho) based alloys; (E) The desorption Van't Hoff plots of $Ti_{1.02}Cr_{1.1}Mn_{0.3}Fe_{0.6}$ and $Ti_{1.0}2Cr_{1.1}Mn_{0.3}Fe_{0.6}RE_{0.03}$ (RE = La, Ce, Ho) based alloys [37].

desorption plateau pressure. Among the studied alloys, the $Ti_{1.02}Cr_{1.1}Mn_{0.3}Fe_{0.6}La_{0.03}$ alloy shows the best overall properties and can be fully activated at room temperature. As shown in **Figure 6(D)** & **Figure 6(E)**, its hydrogen absorption pressure is 39.31 MPa and 51.27 MPa under 298 K and 318 K, respectively. Its hydrogen storage capacity is up to 1.715 wt.%.

Meanwhile, Sakaki *et al*. [38] After V replaces part of Cr in TiCr2 alloy, the unit cell parameter of the $Ti_{20}Cr_{30}V_{50}$ alloy increases, compared with $Ti_{35}Cr_{55}V_{10}$ alloy. Its hydrogen absorption capacity increases, the hysteresis effect increases, and the hydrogen absorption and desorption platform pressure decreases. For the same reason, the substitution of a smaller amount of Fe or Mn atoms for Cr could potentially lead to a reduction in unit cell size. After element substitution exhibited higher hydrogen storage capacities and lower hydrogen desorption plateau pressures. What's more, adding Zr element with larger atomic radius can increase the unit cell volume of the alloy. Kumar *et al*. [39] found that after Zr adding into the $Ti_{20}Cr_{20-x}Ni_{20}V_{20}Zr_X$alloy, the lattice constant increases, the lattice gap that can accommodate hydrogen atoms in the alloy increases, which causing the activation performance of the alloy effectively being improved and the hydrogen absorption being increased.

In addition, the use of specific heat treatment methods can also make the Ti-Cr alloy absorb more hydrogen, improve its hydrogen storage performance, activation performance and cycling stability. By annealing the material, increasing the annealing temperature or prolonging the annealing time can make the distribution of each alloy element become uniform, improving the hydrogen storage capacity. Changing the heating rate of the annealing stage to improve the activation performance of the material, the PCT curve hydrogen release platform becomes slower and the platform stage becomes wider [40].

2.3.2. Ti-Mnalloy

The Mn-Ti binary phase diagram is depicted in **Figure 7**. There is a wide Laves phase region in the phase diagram, which means that when the stoichiometric ratio of Ti-Mn alloy deviates from $TiMn_2$ obviously, the alloy is still a single Laves phase structure, which is prone to hydrogen desorption [41]. Among other Ti-Mn binary alloys, the $TiMn_2$ alloy has a poor hydrogen storage performance, while $TiMn_{1.5}$ is the best for storing hydrogen at room temperature, with storing up to 1.8 wt.%.

Ti-Mn hydrogen storage alloys exhibit notable features such as a relatively high hydrogen storage capacity, straightforward activation process, rapid hydrogen absorption and desorption rates, a broad range of adjustable platform pressures for hydrogen absorption and desorption, as well as excellent cycle performance. Most of the existing studies use element replacement method, specific heat treatment method and other methods to optimize $TiMn_2$-based hydrogen storage alloy to improve the practical application possibility of the material.

Cr replacing Mn in $TiMn_2$-based alloy can effectively reduce the hysteresis

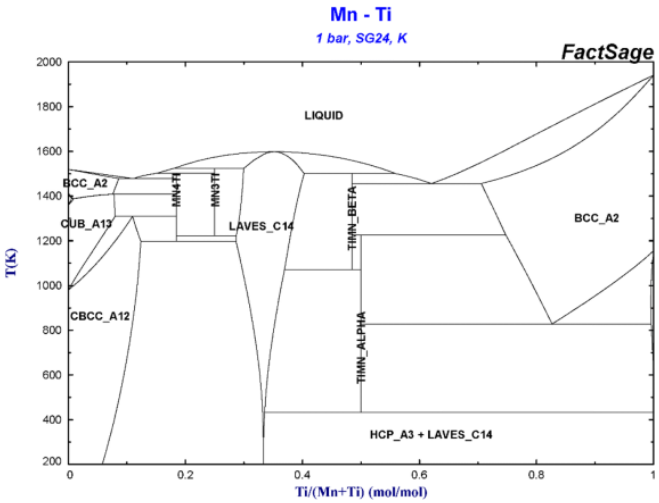

Figure 7. Binary phase diagram of Ti-Mn [41].

effect of hydrogen uptake and desorption platform in $TiMn_2$-based alloy. The platform of hydrogen adsorption and desorption becomes shorter, and the volume of the alloy unit cell increases, but the hydrogen uptake capacity decreases. Zhou *et al*. [42] explored two serious of $Ti_{1-x}Zr_xMn_{1.1}Cr_{0.7}V_{0.2}$ and $Ti_{0.95}Zr_{0.05}Mn_{1.8-y}CryV_{0.2}$ alloys, whose element uniform distributed and determined as only a single phase of C14-type.Substituting Ti with Zr resulted in an enhancement of the hydrogen storage capacity of the alloy, accompanied by a notable decrease in platform pressure. The addition of Zr element enhances hydrogen storage performance by altering hydrogen affinity, increasing alloy crystal lattice constant, reducing hydrogen absorption pressure, and improving platform slope. Substitution of Mn with Cr resulted in a reduction in the hydrogen absorption and desorption kinetics of the material, leading to a slight decrease in hydrogen storage capacity to 1.78 wt.%. Additionally, the pressure required for hydrogen desorption at 363K temperature was measured at 9.37 MPa.

Ma *et al*. [43] investigated $Ti_{1-x}Sc_xMn_{1.6}V_{0.4}$ alloy that with addition of Sc, it exceedingly improved hydrogen activation and storage properties. With the increase of Sc content, the unit cells of the material expanded. According to the mechanism of hydrogen cracking, the activation characteristics of the material are related to its particle size. After the addition of Sc element, the problem that the particle size is too small to be activated is solved, and the material is easily activated at this time. Meanwhile, according to Zhu *et al*. [44] research, Sc substitution for Ti causes the chemical composition's changes of the BCC phase and the formation of second phases, which would cause the plateau pressure of $TiMn_{10}V_{40}Cr_{10}Sc_X$ alloy system too low.

Chen *et al*. [45] explored that with adding the V element, the pressure hysteresis of the hydrogen uptake and discharge platform is weakened, considering to a polycrystalline phase containing C14phase and BCC phase (as shown in **Figure 8(A)**). The addition of V element to the alloy system can effectively reduce the pressure of the hydrogen uptake and discharge platform without reducing the

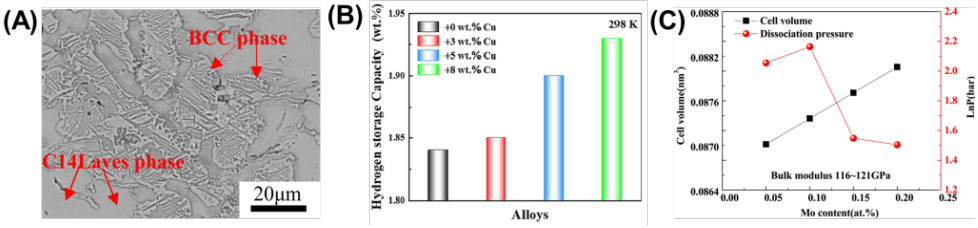

Figure 8. (A) Microstructure of cast $Ti_{29}Mn_{46}V_{25}$ [45]; (B) the maximum hydrogen storage capacity of $Ti_{0.8}Zr_{0.2}Mn_{0.92}Cr_{0.87}Fe_{0.21}$ + xCu (x = 0, 3, 5 and 8 wt.%) alloys at 298 K [46]; (C) Dependence of Cell volume, dissociation pressure and Mo content [47].

hydrogen storage capacity of the $TiMn_2$-based alloy. Cu can reduce the pressure of hydrogen absorption and desorption platform of $TiMn_2$-based alloy, with the hydrogen storage capacity increasing. As Qiao *et al.* [46] reported that with Cu doping, the lattice volume of the alloy material increases, and the activation performance and hysteresis of the material are improved, which is exhibited in **Figure 8(B)**. Yan *et al.* [47] found that addition of a small amount of Mo can improve the hydrogen storage capacity of $TiMn_2$-based alloys, and a small amount of Mo replacing Mn can increase the storage capacity and related cell volume.

In addition, doped oxides also alter the total hydrogen storage properties. Li *et al.* [48] found that the appropriate addition of SiO_2would maintain excellent cyclic stability. But when excessive SiO_2 (~2.0 wt.%) was added, the hydrogen storage plateau slope of the alloy increased sharply, and the hydrogen storage capacity decreased. It is ascribed that the formation of ZrO_2 phase and the doping of Si with the SiO_2 content increase, resulting in the lattice constant of the alloy increasing and the plateau pressure decreasing.

In addition to the above regulation of the types and composition of the alloy elements, the hydrogen storage performance of $TiMn_2$-based hydrogen storage alloy can also be improved by pretreatment. By utilizing the high-energy ball milling method, it becomes possible to transform the $TiMn_2$-based hydrogen storage alloy from particles of micrometer size to particles of nanometer size. This transformation results in an increased surface area for contact between the metalalloy and hydrogen, leading to enhanced hydrogen storage capabilities. Furthermore, the ball milling process effectively eliminates surface contamination present on the raw material, revealing a newer and fresher surface. It is worth noting that these improvements are accomplished without any modifications to the phase structure of the alloy [49]. The capacity of hydrogen storage in TIMN2-based alloys can be altered through various heat treatment methods [50]. By subjecting the material to heat treatment, the grain structure of the hydrogen storage alloy can be refined, reducing defects and creating more sites for hydrogen acceptance [51]. The uneven distribution of elements in the bulk phase of the alloy, which causes the platform stage in the hydrogen storage and release process, can be eliminated through heat treatment. As a result, the material's platform becomes flatter, the hydrogen storage platform widens, and the overall hydrogen storage capacity increasing [8].

3. Conclusion and Prospect

As shown in **Table 1**, There are various hydrogen storage systems, among which Ti-based hydrogen storage alloy is considered to be one of the future hydrogen storage materials that can be used in practical large-scale applications. Ti-based

Table 1. Summary of data related to hydrogen storage performance of titanium based hydrogen storage alloys.

alloy	hydrogen capacity (wt.%)	Hydrogen absorption plateaupressure (MPa)	Hydrogen desorption plateaupressure (MPa)	Hydrogen release enthalpy (kJ/mol H_2)
TiFe [52]	1.50	0.64 (298 K)	0.41 (298 K)	28.1
$TiF_{e0.95}Mn_{0.05}$ [31]	1.60	1.05 (328 K)	0.4 (298 K)	32.3
$TiFe_{0.90}Mn_{0.1}$ [31]	1.40	0.95 (328 K)	0.30 (298 K)	31.5
$TiFe_{0.85}Mn_{0.15}$ [31]	1.28	0.62 (328 K)	0.26 (298 K)	29.3
$TiFe_{0.8}Ni_{0.2}$ [52]	1.30	0.06 (298 K)	0.01 (298 K)	41.2
$Ti_{45.4}Fe_{45.4}Zr_{2.55}Mn_{6.55}$ [32]	1.66	0.50 (303 K)	0.20 (303 K)	23.4
$Ti_{44.5}Fe_{44.5}Zr_{2.5}Mn_{6.5}Nb_2$ [32]	2.04	0.39 (303 K)	0.18 (303 K)	23.1
$Ti_{44.5}Fe_{44.5}Zr_{2.5}Mn_{6.5}Nb_2$ [32]	2.11	0.26 (303 K)	0.12 (303 K)	26.6
$Ti_{41.8}Fe_{41.8}Zr_{2.35}Mn_{6.05}Nb_8$ [32]	2.07	0.23 (303 K)	0.11 (303 K)	27.1
$Ti_{52.63}Fe_{45.26}Mn_{1.05}Cu_{1.05}$ [53]	1.83	0.50 (298 K)	0.06 (298 K)	37.6
$TiCr_{1.8}$ [52]	2.43	0.23 (298 K)	0.11 (298 K)	20.2
$TiMn_{1.5}$ [52]	1.86	0.90 (298 K)	0.84 (298 K)	28.7
$TiMn_{1.4}V_{0.62}$ [52]	2.15	0.50 (298 K)	0.36 (298 K)	28.6
$Ti_{34.9}Mn_{42.5}V_{17.3}(Zr_{0.6}Cr_{1.4}Fe_{3.2})$ [41]	1.32	0.60 (300 K)	0.47 (300 K)	29.9
$Ti_{32}Mn_{46.8}V_{14}Ni_{6.1}(Zr_{0.7}Cr_{1.2}Fe_{3.2})$ [41]	1.64	2.55 (300 K)	1.89 (300 K)	26.3
$Ti_{33.3}Mn_{44.1}V_{15.3}(Zr_{0.6}Cr_{1.6}Fe_{4.9})$ [41]	1.30	2.21 (298 K)	1.76 (298 K)	28.7
$Ti_{28.6}Mn_{50.9}V_{11.1}(Zr_{0.7}Cr_{4.5}Fe_{4.1})$ [41]	1.39	7.79 (297 K)	4.68 (297 K)	24.8
$Ti_{0.95}Mn_{1.3}Zr_{0.05}Cr_{0.5}V_{0.2}$ [42]	1.84	4.90 (303 K)	2.73 (303 K)	21.1
$Ti_{0.95}Mn_{1.1}Zr_{0.05}Cr_{0.7}V_{0.2}$ [42]	1.81	3.55 (303 K)	2.49 (303 K)	21.2
$Ti_{0.95}Mn_{0.9}Zr_{0.05}Cr_{0.9}V_{0.2}$ [42]	1.78	2.64 (303 K)	2.30 (303 K)	21.6
$Ti_{0.95}Mn_{1.6}Sc_{0.05}V_{0.4}$ [43]	2.20	0.65 (293 K)	0.36 (293 K)	12.0
$Ti_{0.85}Mn_{1.6}Sc0_{.15}V_{0.4}$ [43]	2.26	0.13 (293 K)	0.07 (293 K)	13.9
$Ti_{0.80}Mn_{1.6}Sc_{0.20}V_{0.4}$ [43]	2.27	0.06 (293 K)	0.04 (293 K)	15.1
$Ti_{0.8}Mn_{0.92}Zr_{0.2}Cr_{0.87}Fe_{0.21}$ + 0Cu [46]	1.84	0.37 (298 K)	0.20 (298 K)	20.1
$Ti_{0.8}Mn_{0.92}Zr_{0.2}Cr_{0.87}Fe_{0.21}$ + 3Cu [46]	1.85	0.35 (298 K)	0.21 (298 K)	25.5
$Ti_{0.8}Mn_{0.92}Zr_{0.2}Cr_{0.87}Fe_{0.21}$ + 5Cu [46]	1.90	0.34 (298 K)	0.26 (298 K)	26.4
$(Ti_{0.85}Zr_{0.15})_{1.1}Cr_{0.95}Mo_{0.05}Mn$ [47]	1.76	1.02 (303 K)	0.78 (303 K)	26.0
$(Ti_{0.85}Zr_{0.15})_{1.1}Cr_{0.90}Mo_{0.10}Mn$ [47]	1.75	1.06 (303 K)	0.87 (303 K)	19.0
$(Ti_{0.85}Zr_{0.15})_{1.1}Cr_{0.80}Mo_{0.20}Mn$ [47]	1.65	0.53 (303 K)	0.45 (303 K)	16.0

hydrogen storage alloy has the advantages of low price and easy modification. However, the traditional Ti-based hydrogen storage alloy is difficult to meet the existing hydrogen storage requirements. Machine learning and simulation calculation methods are used to guide the material optimization scheme. Most of the existing studies use methods such as addition or replacement of elements, surface treatment and heat treatment to improve the comprehensive hydrogen storage performance of materials by changing the components of hydrogen storage alloys or improving the microstructure of hydrogen storage alloys.

However, no comprehensive method has been discovered to enhance all the hydrogen storage properties of alloys simultaneously. Therefore, it is necessary to conduct more in-depth research and discussion on the hydrogen storage principle and the atomic structure of Ti-based hydrogen storage alloy to obtain a clearer structure-activity relationship between material structure and performance, which will play a pointing role in the future optimization of Ti-based hydrogen storage alloy.

Future research should be deeply combined with machine learning, focusing on the development of Ti-based hydrogen storage alloys with high hydrogen storage capacity, fast hydrogen storage and discharge process rate, and high safety, so as to meet the needs of large-scale practical application. At the same time, attention should be paid to the development of supporting facilities and technologies related to hydrogen storage alloys, and a practical and efficient hydrogen storage system should be developed.

Conflicts of Interest

The authors declare no conflicts of interest regarding the publication of this paper.

References

[1] Lange, J.P. (2021) Towards Circular Carbo-Chemicals—The Metamorphosis of Petrochemicals. *Energy Environ. Sci*, **14**, 4358-4376. https://doi.org/10.1039/D1EE00532D

[2] Smith, J.C. and Clark, C. (2019) The Future's Energy Mix: The Journey to Integration [Guest Editorial]. *IEEE Power and Energy Magazine*, **17**, 19-23. https://doi.org/10.1109/MPE.2019.2933283

[3] Dragoon, K., Iliceto, A., Korpas, M., Markussen, P., Pivovar, B., Ruth, M., Westlake, B. and Endler, E. (2022) Hydrogen as Part of a 100% Clean Energy System: Exploring Its Decarbonization Roles. *IEEE Power and Energy Magazine*, **20**, 85-95. https://doi.org/10.1109/MPE.2022.3167598

[4] Andrews, C.J. and Weiner, S.A. (2004) Visions of a Hydrogen Future. *IEEE Power and Energy Magazine*, **2**, 26-34. https://doi.org/10.1109/MPAE.2004.1269614

[5] Mazloomi, K. and Gomes, C. (2012) Hydrogen as an Energy Carrier: Prospects and Challenges. *Renewable and Sustainable Energy Reviews*, **16**, 3024-3033. https://doi.org/10.1016/j.rser.2012.02.028

[6] Kumar, A., Muthukumar, P., Sharma, P. and Kumar, E.A. (2022) Absorption Based Solid State Hydrogen Storage System: A Review. *Sustain. Energy Technol. Assess*,

52, 102204. https://doi.org/10.1016/j.seta.2022.102204

[7] Ye, J., Jiang, L., Li, Z., Wang, S., Wang, Q., Luo, M., Wu, Y., Guo, X., Wu, J., Zhang, L., Chen, H. and Wu, R. (2024) Optimization Design of Solid-State Hydrogen Storage Device for Fuel Cell Forklift. *J. Alloy. Compd*, **970**, 172242. https://doi.org/10.1016/j.jallcom.2023.172242

[8] Huang, L.J., Lin, H.J., Wang, H., Ouyang, L.Z. and Zhu, M. (2023) Amorphous Alloys for Hydrogen Storage. *J. Alloy. Compd*, **941**, 168945. https://doi.org/10.1016/j.jallcom.2023.168945

[9] Hu, L., Nan, R., Li, J., Gao, L. and Wang, Y. (2017) Phase Transformation and Hydrogen Storage Properties of an La7.0Mg75.5Ni17.5 Hydrogen Storage Alloy Crystals. https://doi.org/10.3390/cryst7100316

[10] Hu, H., Tang, R., Xiao, H., He, X., Zhou, W., Zhang, X., Ma, C. and Chen, Q. (2023) Development of V-Free BCC Structured Alloys for Hydrogen Storage. *Acs Appl. Energ. Mater*, **6**, 11108-11117. https://doi.org/10.1021/acsaem.3c01934

[11] Yu, H., Li, X. and Zheng, J. (2024) Beyond Hydrogen Storage: Metal Hydrides for Catalysis. *Acs Catal.*, 3139-3157. https://doi.org/10.1021/acscatal.3c05696

[12] Klopčič, N., Grimmer, I., Winkler, F., Sartory, M. and Trattner, A. (2023) A Review on Metal Hydride Materials for Hydrogen Storage. *J. Energy Storage*, **72**, 108456. https://doi.org/10.1016/j.est.2023.108456

[13] German, E., Sandoval, J., Recio, A., Seif, A., Alonso, J.A. and López, M.J. (2023) Supported Metal Nanohydrides for Hydrogen Storage. *Chem. Mat*, **35**, 1134-1147. https://doi.org/10.1021/acs.chemmater.2c03106

[14] Chen, Z., Kirlikovali, K.O., Idrees, K.B., Wasson, M.C. and Farha, O.K. (2022) Porous Materials for Hydrogen Storage. *Chem*, **8**, 693-716. https://doi.org/10.1016/j.chempr.2022.01.012

[15] Guo, J., Li, S., Su, Y. and Chen, G. (2020) Theoretical Study of Hydrogen Storage by Spillover on Porous Carbon Materials. *Int. J. Hydrog. Energy*, **45**, 25900-25911. https://doi.org/10.1016/j.ijhydene.2019.12.146

[16] Saeed, M., Marwani, H.M., Shahzad, U., Asiri, A.M. and Rahman, M.M. (2024) Nanoscale Silicon Porous Materials for Efficient Hydrogen Storage Application. *J. Energy Storage*, **81**, 110418. https://doi.org/10.1016/j.est.2024.110418

[17] Marinelli, M. and Santarelli, M. (2020) Hydrogen Storage Alloys for Stationary Applications. *J. Energy Storage*, **32**, 101864. https://doi.org/10.1016/j.est.2020.101864

[18] Tu, B., Wang, H., Wang, Y., Li, R., Ouyang, L. and Tang, R. (2022) Optimizing Ti-Zr-Cr-Mn-Ni-V Alloys for Hybrid Hydrogen Storage Tank of Fuel Cell Bicycle. *Int. J. Hydrog. Energy*, **47**, 14952-14960. https://doi.org/10.1016/j.ijhydene.2022.03.018

[19] Marques, F., Balcerzak, M., Winkelmann, F., Zepon, G. and Felderhoff, M. (2021) Review and Outlook on High-Entropy Alloys for Hydrogen Storage. *Energy Environ. Sci*, **14**, 5191-5227. https://doi.org/10.1039/D1EE01543E

[20] Shang, H., Zhang, Y., Gao, J., Zhang, W., Wei, X., Yuan, Z. and Li, Y. (2022) Characteristics of Electrochemical Hydrogen Storage Using Ti-Fe Based Alloys Prepared by Ball Milling. *Int. J. Hydrog. Energy*, **47**, 1036-1047. https://doi.org/10.1016/j.ijhydene.2021.10.068

[21] Liu, J., Sun, L., Yang, J., Guo, D., Chen, D., Yang, L. and Xiao, P. (2022) Ti-Mn Hydrogen Storage Alloys: From Properties to Applications. *Rsc Adv*, **12**, 35744-35755. https://doi.org/10.1039/D2RA07301C

[22] Lv, P., Zhong, C., Huang, D., Zhou, X., Liu, Z. and Zhao, R. (2022) Superior An-

ti-Impurity Gas Poisoning Ability and Hydrogen Storage Properties of Ti-Cr Alloy by Introducing Zirconium as Additive. *Int. J. Hydrog. Energy*, **47**, 18772-18785. https://doi.org/10.1016/j.ijhydene.2022.04.041

[23] Hu, J., Zhang, J., Xiao, H., Xie, L., Sun, G., Shen, H., Li, P., Zhang, J. and Zu, X. (2021) A First-Principles Study of Hydrogen Storage of High Entropy Alloy TiZrVMoNb. *Int. J. Hydrog. Energy*, **46**, 21050-21058. https://doi.org/10.1016/j.ijhydene.2021.03.200

[24] Fadonougbo, J.O., Park, K.B., Na, T., Park, C., Park, H. and Ko, W. (2022) An Integrated Computational and Experimental Method for Predicting Hydrogen Plateau Pressures of TiFe1-xMx-Based Room Temperature Hydrides. *Int. J. Hydrog. Energy*, **47**, 17673-17682. https://doi.org/10.1016/j.ijhydene.2022.03.240

[25] Lu, Z., Wang, J., Wu, Y., Guo, X. and Xiao, W. (2022) Predicting Hydrogen Storage Capacity of V-Ti-Cr-Fe Alloy via Ensemble Machine Learning. *Int. J. Hydrog. Energy*, **47**, 34583-34593. https://doi.org/10.1016/j.ijhydene.2022.08.050

[26] Loh, S.M., Grant, D.M., Walker, G.S. and Ling, S. (2023) Substitutional Effect of Ti-Based AB2 Hydrogen Storage Alloys: A Density Functional Theory Study. *Int. J. Hydrog. Energy*, **48**, 13227-13235. https://doi.org/10.1016/j.ijhydene.2022.12.083

[27] Zhou, P., Xiao, X., Zhu, X., Chen, Y., Lu, W., Piao, M., Cao, Z., Lu, M., Fang, F., Li, Z., Jiang, L. and Chen, L. (2023) Machine Learning Enabled Customization of Performance-Oriented Hydrogen Storage Materials for Fuel Cell Systems. *Energy Storage Mater*, **63**, 102964. https://doi.org/10.1016/j.ensm.2023.102964

[28] Suwarno, S., Dicky, G., Suyuthi, A., Effendi, M., Witantyo, W., Noerochim, L. and Ismail, M. (2022) Machine Learning Analysis of Alloying Element Effects on Hydrogen Storage Properties of AB2 Metal Hydrides. *Int. J. Hydrog. Energy*, **47**, 11938-11947. https://doi.org/10.1016/j.ijhydene.2022.01.210

[29] Liu, H., Zhang, J., Sun, P., Zhou, C., Liu, Y. and Fang, Z.Z. (2022) Effect of Oxygen on the Hydrogen Storage Properties of TiFe Alloys. *J. Energy Storage*, **55**, 105543. https://doi.org/10.1016/j.est.2022.105543

[30] Liu, H., Zhang, J., Sun, P., Zhou, C., Liu, Y. and Fang, Z.Z. (2023) An Overview of TiFe Alloys for Hydrogen Storage: Structure, Processes, Properties, and Applications. *J. Energy Storage*, **68**, 107772. https://doi.org/10.1016/j.est.2023.107772

[31] Pati, S., Trimbake, S., Vashistha, M. and Sharma, P. (2021) Tailoring the Activation Behaviour and Oxide Resistant Properties of TiFe Alloys by Doping with Mn. *Int. J. Hydrog. Energy*, **46**, 34830-34838. https://doi.org/10.1016/j.ijhydene.2021.08.041

[32] Liu, H., Zhang, J., Zhou, C., Sun, P., Liu, Y. and Fang, Z.Z. (2023) Hydrogen Storage Properties of Ti-Fe-Zr-Mn-Nb Alloys. *J. Alloy. Compd*, **938**, 168466. https://doi.org/10.1016/j.jallcom.2022.168466

[33] Li, C., Gao, X., Liu, B., Wei, X., Zhang, W., Lan, Y., Wang, H. and Yuan, Z. (2023) Effects of Zr Doping on Activation Capability and Hydrogen Storage Performances of TiFe-Based Alloy. *Int. J. Hydrog. Energy*, **48**, 2256-2270. https://doi.org/10.1016/j.ijhydene.2022.10.098

[34] Ha, T., Kim, J., Sun, C., Lee, Y., Kim, D., Suh, J., Jang, J., Lee, J., Kim, Y. and Shim, J. (2023) Crucial Role of Ce Particles during Initial Hydrogen Absorption of AB-Type Hydrogen Storage Alloys. *Nano Energy*, **112**, 108483. https://doi.org/10.1016/j.nanoen.2023.108483

[35] Zhu, Y., Li, X., Yang, X., Chen, P., Tsui, G.C., Xu, Z., Tang, R., Xiao, F. and Chan, K. (2023) Compositionally Complex Doping for low-V Ti-Cr-V Hydrogen Storage Alloys. *Chem. Eng. J*, **477**, 146970. https://doi.org/10.1016/j.cej.2023.146970

[36] Zhang, Y., Li, C., Zhang, W., Wei, X., Li, J., Qi, Y. and Zhao, D. (2023) Research and

Application of Ti-Mn-Based Hydrogen Storage Alloys. *J. Iron Steel Res. Int*, **30**, 611-625. https://doi.org/10.1007/s42243-022-00905-1

[37] Yao, Z., Liu, L., Xiao, X., Wang, C., Jiang, L. and Chen, L. (2018) Effect of Rare Earth Doping on the Hydrogen Storage Performance of $Ti_{1.02}Cr_{1.1}Mn_{0.3}Fe_{0.6}$ Alloy for Hybrid Hydrogen Storage Application. *J. Alloy. Compd*, **731**, 524-530. https://doi.org/10.1016/j.jallcom.2017.10.075

[38] Xue, X., Ma, C., Liu, Y., Wang, H. and Chen, Q. (2023) Impacts of Ce Dopants on the Hydrogen Storage Performance of Ti-Cr-V Alloys. *J. Alloy. Compd*, **934**, 167947. https://doi.org/10.1016/j.jallcom.2022.167947

[39] Kumar, A., Yadav, T.P. and Mukhopadhyay, N.K. (2022) Notable Hydrogen Storage in Ti-Zr-V-Cr-Ni High Entropy Alloy. *Int. J. Hydrog. Energy*, **47**, 22893-22900. https://doi.org/10.1016/j.ijhydene.2022.05.107

[40] Rong, M., Wang, F., Wang, J., Wang, Z. and Zhou, H. (2017) Effect of Heat Treatment on Hydrogen Storage Properties and Thermal Stability of $V_{68}Ti_{20}Cr_{12}$ Alloy. *Progress in Natural Science*: *Materials International*, **27**, 543-549. https://doi.org/10.1016/j.pnsc.2017.08.012

[41] Nayebossadri, S. and Book, D. (2019) Development of a High-Pressure Ti-Mn Based Hydrogen Storage Alloy for Hydrogen Compression. *Renew. Energy*, **143**, 1010-1021. https://doi.org/10.1016/j.renene.2019.05.052

[42] Zhou, P., Cao, Z., Xiao, X., Zhan, L., Li, S., Li, Z., Jiang, L. and Chen, L. (2021) Development of Ti-Zr-Mn-Cr-V Based Alloys for High-Density Hydrogen Storage. *J. Alloy. Compd*, **875**, 160035. https://doi.org/10.1016/j.jallcom.2021.160035

[43] Ma, P., Li, W. and Wu, E. (2021) Hydrogen Activation and Storage Properties of Laves Phase $Ti_{1-x}Sc_xMn_{1.6}V_{0.4}$ Alloys. *Int. J. Hydrog. Energy*, **46**, 34389-34398. https://doi.org/10.1016/j.ijhydene.2021.08.017

[44] Zhu, J., Ma, L., Liang, F., Wang, L. (2015) Effect of Sc Substitution on Hydrogen Storage Properties of Ti-V-Cr-Mn Alloys. *Int. J. Hydrog. Energy*, **40**, 6860-6865. https://doi.org/10.1016/j.ijhydene.2015.03.149

[45] Chen, X.Y., Chen, R.R., Ding, X., Fang, H.Z., Guo, J.J., Ding, H.S., Su, Y.Q. and Fu, H.Z. (2018) Crystal Structure and Hydrogen Storage Properties of Ti-V-Mn Alloys. *Int. J. Hydrog. Energy*, **43**, 6210-6218. https://doi.org/10.1016/j.ijhydene.2018.02.009

[46] Qiao, W., Yin, D., Zhao, S., Ding, N., Liang, L., Wang, C., Wang, L., He, M. and Cheng, Y. (2023) Effects of Cu Doping on the Hydrogen Storage Performance of Ti-Mn-Based, AB2-Type Alloys. *Chem. Eng. J*, **465**, 142837. https://doi.org/10.1016/j.cej.2023.142837

[47] Yan, Y., Li, Z., Wu, Y. and Zhou, S. (2022) Hydrogen Absorption-Desorption Characteristic of $(Ti_{0.85}Zr_{0.15})_{1.1}Cr_{1-x}$MoxMn Based Alloys with C14 Laves Phase. *Progress in Natural Science*: *Materials International*, **32**, 143-149. https://doi.org/10.1016/j.pnsc.2022.03.001

[48] Li, J., Hu, H., Xiao, H., Ma, C., Yi, L. and Chen, Q. (2023) Effect of SiO_2-Doped on Microstructural Evolution and Hydrogen Storage Performances of AB2 Type Alloy. *J. Alloy. Compd*, **950**, 169893. https://doi.org/10.1016/j.jallcom.2023.169893

[49] Shang, H., Sheng, P., Li, J., Zhang, W., Zhang, X., Guo, S., Li, Y. and Zhang, Y. (2023) Characteristics of Hydrogen Storage of As-Milled TiFe-Based Alloys. *Int. J. Hydrog Energy*. https://doi.org/10.1016/j.ijhydene.2023.06.325

[50] Semboshi, S., Masahashi, N., Konno, T.J., Sakurai, M. and Hanada, S. (2004) Composition Dependence of Hydrogen Absorbing Properties in Melt Quenched and Annealed $TiMn_2$ Based Alloys. *J. Alloy. Compd*, **379**, 290-297.

https://doi.org/10.1016/j.jallcom.2004.02.045

[51] Zhang, Q.A., Lei, Y.Q., Yang, X.G., Ren, K. and Wang, Q.D. (1999) Annealing Treatment of AB2-Type Hydrogen Storage Alloys: I. Crystal Structures. *J. Alloy. Compd*, **292**, 236-240. https://doi.org/10.1016/S0925-8388(99)00485-5

[52] Sandrock, G. (1999) A Panoramic Overview of Hydrogen Storage Alloys from a Gas Reaction Point of View. *J. Alloy. Compd*, **293-295**, 877-888. https://doi.org/10.1016/S0925-8388(99)00384-9

[53] Dematteis, E.M., Cuevas, F. and Latroche, M. (2021) Hydrogen Storage Properties of Mn and Cu for Fe Substitution in $TiFe_{0.9}$ Intermetallic Compound. *J. Alloy. Compd*, **851**, 156075. https://doi.org/10.1016/j.jallcom.2020.156075